Optical-Model Analysis of Proton Elastic Scattering in the Range of 9 to 22 MeV

F. G. PEREY
Oak Ridge National Laboratory Oak Ridge, Tennessee*
(Received 18 March 1963)

For incident proton energies between 9 to 22 MeV, 35 elastic scattering angular distributions have been analyzed with the optical model using a least-square criteria over the complete angular range of the data. The observed increase of the real well depth as a function of mass number is explained by the presence of a nuclear symmetry term in the potential and by the momentum dependence of the potential. The polarization and reaction cross-section data are in good agreement with the calculations. The effect of core excitations on the parameters of the optical model are studied, and the relative importance of volume and surface imaginary potentials is discussed. Formulas are given to obtain the value of the parameters of the optical model as a function of mass number and energy.

I. INTRODUCTION

IN this paper an optical-model analysis is made of many proton elastic scattering angular distributions, for elements heavier than Al, with incident proton energies between 9 and 22 MeV. The aim is to find smooth trends in the parameters as a function of mass number and energy. The parameters of the potential were adjusted until a least-square fit to the data was obtained over the complete angular range.

The optical model has been used very successfully[1] in the analysis of elastic scattering of nucleons by nuclei. For neutrons, with an incident energy below 25 MeV, it has been possible to find a set of optical-model parameters, independent of mass number, which vary smoothly as a function of energy.[2] Recently, this energy dependence has been explained in terms of a simple nonlocality of the potential.[3] The proton data is, in general, more precise and should provide a more stringent test of the model. However, most systematic analyses[4] of the proton elastic-scattering data have neglected the spin-orbit potential which leads to polarization in the elastic scattering. Although the addition of the spin-orbit potential does not affect greatly the calculated cross sections at forward angles, it modifies them appreciably at large angles. As a result, most analyses have only attempted to get approximate agreement with the data at backward angles. The early studies also failed to reproduce the data for light nuclei. However, recently, very good agreement has been obtained for the scattering from carbon[5] and oxygen[6] as a function of energy.

In order to fit the data very precisely one may need to introduce more parameters in the model than the usual complex Saxon potential. It then becomes difficult to obtain an unambiguous set of parameters when a single angular distribution is used.[7] The optical model is a very crude representation of the many-body problem and to reproduce the data, some fluctuation in the parameters is expected as a function of mass number. However, if the optical model is to be a useful description of elastic scattering results, the trend of the parameters as a function of mass number and energy should be smooth.

The wave functions from the optical model are now frequently used in the analysis of nuclear reactions, where the transition amplitudes are calculated in the distorted-wave Born approximation. It is of great interest to find out if the optical-potential parameters needed in those calculations are the same as those needed to explain the elastic scattering data.

In Sec. II the various criteria used in the analysis and the selection of adjustable parameters are discussed. The results, corresponding to a particular set of geometrical parameters for the potential, are presented in Sec. III and a simple formula is established for the variation of the potential depths as a function of mass number and energy. The effect of core excitations on the parameters, the evidence for the nuclear symmetry term of the potential, and the relative importance of volume and surface imaginary potential are discussed in Sec. IV.

II. CHOICE OF MODEL AND CRITERIA FOR THE ANALYSIS

A. Definition of the Potentials

The optical model used is defined by the sum of the following potentials:

1. Central potential,

real part $-V_S f(r,r_{0S},a_S)$

imaginary part $-W_S f(r,r_{0I},a_I)+4a_I W_D \frac{d}{dr} f(r,r_{0I},a_I)$.

* Operated by Union Carbide Corporation for the U. S. Atomic Energy Commission.

[1] H. Feshbach, Ann. Rev. Nucl. Sci. **8**, 49 (1958). (This paper gives an extensive review of the early optical model analyses.)

[2] F. Bjorklund and S. Fernbach, Phys. Rev. **109**, 1295 (1958).

[3] F. Perey and B. Buck, Nucl. Phys. **32**, 353 (1962).

[4] M. A. Melkanoff, J. S. Nodvik, D. S. Saxon, and R. D. Woods, Phys. Rev. **106**, 793 (1957); A. E. Glassgold, W. B. Cheston, M. L. Stein, S. B. Schuldt, and G. W. Erickson, *ibid.* **106**, 1207 (1957); A. E. Glassgold and P. J. Kellogg, *ibid.* **107**, 1372 (1957); A. E. Glassgold and P. J. Kellogg, *ibid.* **109**, 1291 (1958).

[5] J. S. Nodvik, C. B. Duke, and M. A. Melkanoff, Phys. Rev. **125**, 975 (1962).

[6] C. B. Duke, Phys. Rev. **129**, 681 (1963).

[7] R. B. Easlea, Proc. Phys. Soc. (London) **78**, 1285 (1961).

2. Spin-orbit potential,

$$\boldsymbol{\sigma}\cdot\mathbf{l}\left(\frac{\hbar}{m_\pi c}\right)^2\frac{V_{S0}}{r}\frac{d}{dr}f(r,r_{0S},a_S).$$

3. Coulomb potential,

$$\frac{Ze^2}{2R_c}\left(3-\frac{r^2}{R_c^2}\right)\quad\text{for}\quad r\leqslant R_c$$

$$\frac{Ze^2}{r}\qquad\text{for}\quad r>R_c.$$

The function $f(r,r_0,a)$ is the usual Saxon form factor,

$$f(r,r_0,a)=\{1+\exp[(r-r_0A^{1/3})/a]\}^{-1},$$

where A is the atomic mass of the nucleus in atomic mass units.

The imaginary potential is composed of a volume part W_S and a surface part W_D [the factor $4a_I$ being required so that the surface form factor, $4a_Idf/dr$, has unity for its maximum value]. The Coulomb potential written would be that produced by a uniform charge distribution of radius R_c. Since the results are not sensitive to the value of R_c, throughout this analysis it is kept fixed at $R_c=1.25A^{1/3}$; in most cases this is also the radius at which the real part of the potential has fallen to half its maximum value. The model as defined contains 8 parameters. The method of solving Schrödinger's equation is similar to that of Buck *et al.*[8]; the problem was coded for the IBM 7090 at Oak Ridge.

Fitting Criteria Used

The quantity χ^2, defined as

$$\chi^2=\frac{1}{N}\sum_{i=1}^{N}\left(\frac{\sigma_{\rm th}(\theta_i)-\sigma_{\rm exp}(\theta_i)}{\Delta\sigma_{\rm exp}(\theta_i)}\right)^2,$$

was selected to compare objectively and quantitatively the fits as a function of the optical-potential parameters. Here, $\sigma_{\rm th}$ and $\sigma_{\rm exp}$ are the calculated and experimental values, respectively, of the cross section at θ_i, and $(\Delta\sigma_{\rm exp})^{-2}$ the corresponding weight of $\sigma_{\rm exp}$; generally $\Delta\sigma_{\rm exp}$ is taken to be the experimental error.

The above expression for χ^2 assumes that the errors are uncorrelated at each data point. However, most of the errors in proton elastic-scattering results do not come from the statistics on the number of points in the elastic peak, but rather, from measurements of target thickness, target angle, counter solid angle, total charge for each run, etc. Such errors are sometimes correlated is a different manner over the angular range of the data. In most cases it would be very difficult to take into account properly such correlated errors and we have for simplicity taken the above criterion for the goodness of fit of the optical model to the data. Such a criterion has been used before in optical-model analyses[5,6,9]; however, some comments, based on the author's subjective evaluation of the fit, will be made on the use of χ^2 as a measure of goodness of fit.

(a) The numerical value of χ^2 does not give a very good idea of the fit; the general shape of the angular distribution must be known also. For fits which are equally satisfactory in a subjective sense, the values of χ^2 required are found to be roughly proportional to the number of oscillations in the angular distribution as well as their amplitude. The "phase" of the theoretical oscillations with respect to the experimental ones is very important in judging a fit; χ^2 does not give any direct indication of this phase.

(b) When χ^2 is "small," its variation reflects quite closely the subjective, visual estimate of the variation of the goodness of fit when the theoretical curves are plotted with the data, but χ^2 is much more sensitive than the eye. If the curve has little structure, a change of the order of 20% in χ^2 is required before the fit can be said to have significantly changed visually.

(c) When χ^2 is "large," then it fails completely to give an idea of the badness of fit. Higher moments of the data with respect to the theoretical predictions would be required to give a quantitative measure of the fit. In the final analysis reported here, none of the χ^2 is large in this sense.

Values of χ^2 will be given in this paper but the author has found it only meaningful to compare them for one element at a given energy when the parameters are changed.

The present analysis was made possible by using an automatic parameter search code in conjunction with the optical-model code. The search code minimizes χ^2 with respect to any desired number of the parameters. Such a procedure is now frequently used in optical-model analyses[5,6] and permits a detailed study of the parameter space. The χ^2 surface varies vary much with element, energy, different choices of the weights, $\Delta\sigma_{\rm exp}$, and finally with the model used (for instance, whether one uses volume or surface imaginary potentials). Frequently, the automatic search ends up in a secondary minimum or valley of the χ^2 surface in parameter space, particularly when the number of parameters varied is large. In most of the final results reported here, only V_S and W_D were varied by the search code and the χ^2 surface is relatively smooth. The starting values of the parameters bias the search code to find a minimum in the neighborhood of those values. It was found that some of the data seemed to indicate invariances of the type $V_SR_S^n=\text{const}$ and $W_Da_D=\text{const}$, while others did not; such invariances frequently appear when χ^2 is large in the sense discussed above.

[8] B. Buck, R. N. Maddison, and P. E. Hodgson, Phil. Mag. **5**, 1181 (1960).

[9] J. S. Nodvik and D. S. Saxon, Phys. Rev. **117**, 1539 (1960).

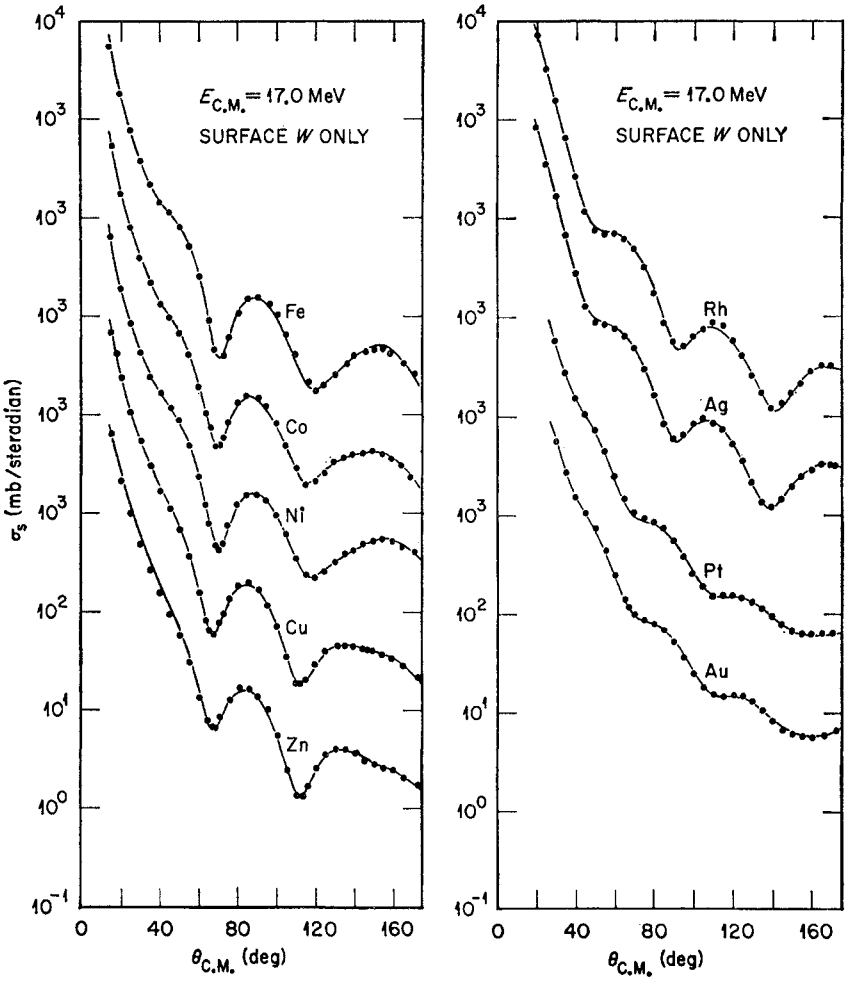

FIG. 1. Fit to the 17-MeV data. Only surface imaginary potential is used and all the parameters of the model were adjusted to obtain a minimum value of χ^2 for each angular distribution. The parameters corresponding to the curves are in Table I.

Choice of Free Parameters

It is generally possible to fit the data very well by allowing all the parameters to vary; however, their values then show fairly large fluctuations from nucleus to nucleus and very little, if any, trend as a function of mass number or energy, although in most cases the values are physically reasonable. As an example, Fig. 1 gives the fits to the 17-MeV data of Dayton and Schrank,[10] for which the parameters are given in Table I; note that only a surface imaginary potential is used. These "best-fit" parameters do not tell us much because of the large fluctuations. It was hoped that at some sacrifice in the quality of fits, some of the parameters could be fixed and then the others would show system-

TABLE I. Parameters corresponding to the fits of Fig. 1. The parameters were all simultaneously varied by the search code and only surface imaginary potential used.

	Fe	Co	Ni	Cu	Zn	Rh	Ag	Pt	Au
V_S (MeV)	48.37	47.64	47.59	45.67	44.52	57.66	55.59	53.61	58.78
r_{0S} (F)	1.238	1.245	1.251	1.301	1.318	1.150	1.172	1.291	1.199
a_S (F)	0.690	0.739	0.677	0.668	0.667	0.687	0.746	0.522	0.654
W_D (MeV)	12.20	13.27	12.50	17.66	18.37	8.206	12.09	23.84	9.918
r_{0I} (F)	1.284	1.282	1.245	1.305	1.280	1.263	1.261	1.206	1.217
a_I (F)	0.456	0.433	0.414	0.343	0.364	0.738	0.593	0.389	0.704
V_{S0} (MeV)	8.76	10.32	9.77	8.02	8.57	8.16	7.18	7.41	9.42
σ_R (mb)	1037.0	1079.0	974.0	1035.0	1080.0	1268.0	1234.0	918.0	1051.0
χ^2	1.21	1.28	0.69	0.505	3.46	0.648	0.812	0.679	0.837

[10] I. E. Dayton and G. Schrank, Phys. Rev. **101**, 1358 (1956).

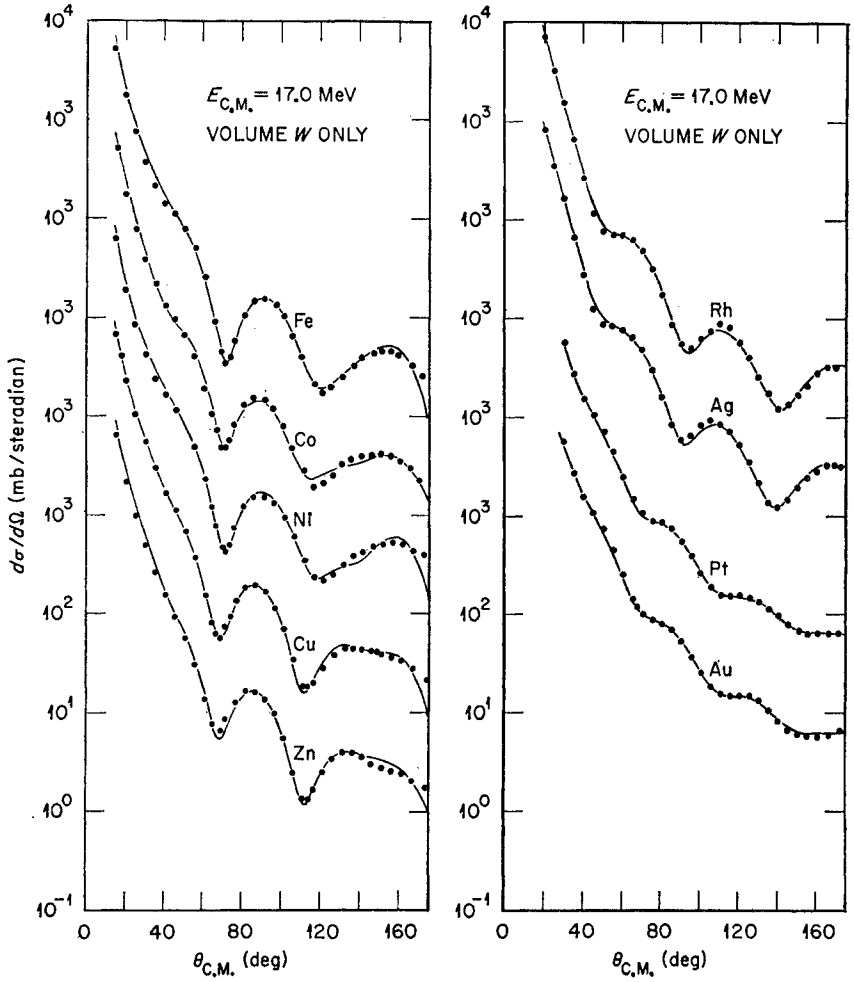

FIG. 2. Fit to the 17-MeV data. Only volume imaginary potential is used and all the parameters of the model were adjusted to obtain a minimum value of χ^2 for each angular distribution. The parameters corresponding to each curve are given in Table II.

atic trends, and maybe some of the fluctuations could be interpreted in terms of nuclear structure or reaction mechanism effects. In particular, it was thought that such an analysis might yield evidence on the shape of the imaginary potential and the presence of a nuclear symmetry term.

The neutron analysis of Bjorklund and Fernbach[2] showed that if one uses a pure surface imaginary potential, it is not necessary to vary the strength W_D as a function of A. A nonlocal potential analysis[3] showed that it was not necessary to change W_D much as a function of energy. It was decided, therefore, to try first a survey with no volume imaginary potential, $W_S=0$, and see how the fits are changed as one gradually increases W_S. Alternatively, one could do the analysis with no surface potential, $W_D=0$, and afterward gradually increase it. A preliminary study using pure volume absorption ($W_D=0$) at 17 MeV failed to

TABLE II. Parameters corresponding to the fits of Fig. 2. The parameters were all simultaneously varied by the search code and only volume imaginary potential used.

	Fe	Co	Ni	Cu	Zn	Rh	Ag	Pt	Au
V_S (MeV)	52.86	60.06	52.47	56.14	59.13	58.66	57.07	61.64	60.77
r_{0S} (F)	1.214	1.063	1.217	1.145	1.104	1.144	1.158	1.192	1.190
a_S (F)	0.505	0.759	0.522	0.647	0.700	0.615	0.663	0.548	0.578
W_S (MeV)	7.03	4.92	7.67	4.84	5.28	4.95	5.71	4.76	4.06
r_{0I} (F)	1.387	1.842	1.258	1.686	1.657	1.636	1.540	1.449	1.550
a_I (F)	0.600	0.209	0.589	0.404	0.561	0.600	0.662	0.715	0.657
V_{S0} (MeV)	6.15	6.74	6.85	6.45	6.20	6.99	6.64	9.51	10.03
σ_R (mb)	956.0	1218.0	1005.0	1111.0	1192.0	1253.0	1248.0	982.0	1049.0
χ^2	5.15	7.91	6.63	5.37	7.40	1.61	3.12	0.862	1.00

yield as good fits as with pure surface absorption ($W_S=0$). The results are given in Fig. 2 and the corresponding parameters are given in Table II. Note that with pure surface imaginary potential, for the medium weight elements, the searches always ended with the same parameters (Table I) when started from many different regions of parameter space. This suggests that the χ^2 minimum is the only one in a large region of parameter space and that the corresponding parameters may be physically significant.

There is evidence[11] that in this energy region W_D plays a major role, or at least that the scattering is more sensitive to the surface part of the imaginary potential. The elastic-scattering data for protons on Cu at 9.5 MeV have been extensively analyzed to determine the best optical-model parameters.[7,9,12] Using a complex Saxon potential Nodvik and Saxon[9] could fit the differential cross section very well with a range of radii. The reaction cross section, σ_R, however, increased with radius and the authors pointed out that a measurement of σ_R would help in determining the best radius. The maximum value of σ_R which they found was 720 mb for a radius parameter $r_{0S}=1.30$ F. The reaction cross section has now been measured by several groups,[13–17] and their results are given in Table III. Since the value of σ_R was much larger than the one calculated by Nodvik and Saxon, Easlea[7] reanalyzed the data by allowing both volume and surface imaginary potentials in his optical model. He found an improvement in the fit at forward angles and was able to raise the reaction cross section to 920 mb using only a surface imaginary potential. For lower σ_R, which are still acceptable, he concludes that the data indicate a ratio of surface-to-volume imaginary potential of at least 2 to 1. Hodgson,[12] however, analyzing the same data but allowing the radius of the imaginary potential to be bigger than the real potential, finds that he can fit the data just as well but needs only a volume imaginary potential. The analyses of Hodgson and Easlea did not use automatic search codes and also constrained some of the parameters to be the same in both the real and the imaginary part of the potential. As soon as one gives up the simple model of a complex Saxon potential, there does not seem to be any compelling reason to keep some of the real and imaginary parameters the same, since the minimum number of parameters is 3 per potential. Our own analysis of the same data, but considering also the polarization[18] (which was not available when Easlea did his analysis), and allowing all the parameters to be varied, shows that the fit to the elastic-scattering angular distribution is the same whether one uses pure volume or pure surface-imaginary potentials. However, the polarization is better fitted with pure surface-imaginary potential. The reaction cross section in all cases is within the experimental errors. In Table IV are some of the solutions found and in Fig. 3 the results for the extreme cases of pure surface and pure volume imaginary potentials. It should be mentioned that Easlea's parameters for pure surface absorption gave a good fit to the polarization and that Hodgson did not try to fit the polarization in detail.

TABLE III. Measured reaction cross sections for natural copper.

Energy (MeV)	9.0[a]	9.3[b]	9.85[c]	9.85[d]	10.0[e]
σ_R (mb)	895±80	930±70	910±60	865±60	816±40

[a] See Ref. 16. [b] See Ref. 15. [c] See Ref. 13. [d] See Ref. 14. [e] See Ref. 17.

It was decided to try to fix the form factors at some value and study the variations of the well depths. It is well known from previous optical analyses that the radius parameter r_{0S} can be varied somewhat around 1.25 F without affecting the fits, provided V_S is adjusted simultaneously. Similarly, a_S can also be varied around a value of 0.65F. In order to be able to compare directly the potentials for neutrons and protons, it was thought convenient to keep r_{0S} and a_S at the same values as Bjorklund and Fernbach,[2]

$$r_{0S}=1.25 \text{ F}$$

and

$$a_S=0.65 \text{ F}.$$

For the imaginary potential, in view of the many uncertainties involved and discussed above, it was decided to try to keep them also as for neutrons;

$$r_{0I}=1.25 \text{ F}, \qquad a_I=0.47 \text{ F}.$$

TABLE IV. Parameters obtained by searching on the 9.4-MeV data for Cu (See Refs. 15 and 18). The fits corresponding to the cases where $W_S=0$ and $W_D=0$ are given in Fig. 3.

V_S (MeV)	52.60	50.01	49.62
r_{0S} (F)	1.209	1.274	1.303
a_s (F)	0.794	0.698	0.596
W_S (MeV)	0.0	4.61	6.19
W_D (MeV)	11.49	4.00	0.0
r_{0I} (F)	1.431	1.547	1.451
a_I (F)	0.457	0.252	0.600
V_{S0} (MeV)	6.70	6.14	5.81
σ_R (mb)	919.0	887.0	864.0
χ_σ^2	0.422	0.400	0.545
χ_P^2	1.15	3.00	4.44

[11] P. E. Hodgson, in *Proceedings of the Rutherford Jubilee International Conference, Manchester, 1961*, edited by J. E. Birks (Heywood and Company, Ltd., Manchester, 1961).
[12] P. E. Hodgson (to be published).
[13] V. Meyer and N. M. Hintz, Phys. Rev. Letters **5**, 207 (1960).
[14] R. D. Albert and L. F. Hansen, Phys. Rev. Letters **6**, 13 (1961); Phys. Rev. **123**, 1749 (1961).
[15] G. W. Greenlees and O. N. Jarvis, Proc. Phys. Soc. (London) **78**, 1275 (1961).
[16] R. F. Carlson, R. M. Eisberg, R. H. Stokes, and T. H. Short, Nucl. Phys. **36**, 511 (1962).
[17] B. Wilkins and G. Igo, Phys. Rev. **129**, 2198 (1963).
[18] A. B. Robbins, K. A. Grotowski, and G. W. Greenlees, in *Proceedings of the Rutherford Jubilee International Conference, Manchester, 1961*, edited by J. E. Birks (Heywood and Company Ltd., Manchester, 1961).

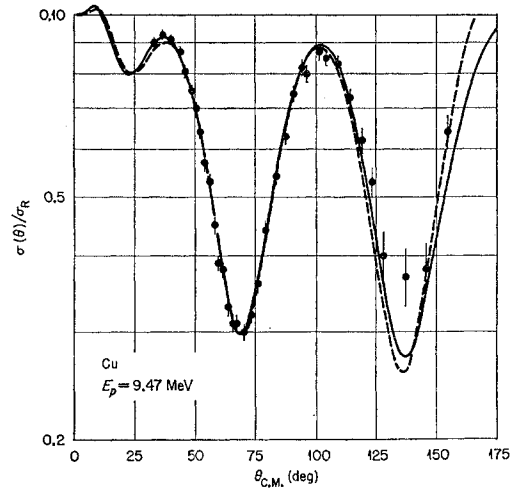

(a)

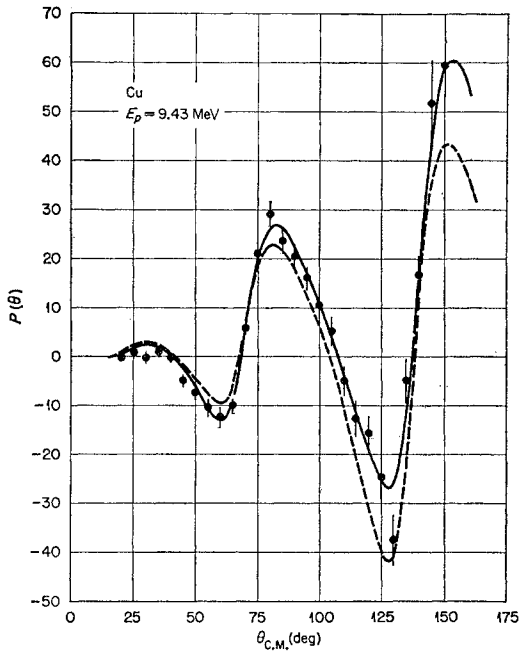

(b)

FIG. 3. Fit to the 9.5-MeV data on Cu. All the parameters of the model were allowed to vary to obtain a minimum value of χ^2. For the full curve only a surface imaginary potential is used and for the dashed curve only a volume imaginary potential. The parameters of the model for each curve are given in Table IV.

Bjorklund and Fernbach used a Gaussian form factor for the surface potential, having a width of 0.98 F, but our form factor with a_I=0.47F gives very nearly the same shape. Several other sets of geometrical parameters were also tried, but although they gave better results on some of the data, on the average the above set is slightly better. Our investigation was necessarily limited, but it was verified that none of the conclusions arrived at were special to the geometrical parameters selected.

The elastic angular distribution is not very sensitive, in general, to the exact value of V_{SO}, the spin-orbit-potential strength, provided it is around 8 MeV as found from previous analyses. During the present analysis it was found that a slightly lower value of V_{SO} was preferred for the lower energies, and that at 17 and 22 MeV a slightly higher value was better. It was then decided not to search on V_{SO} but to fix it, for all elements at a value of 8.5 MeV for 17- and 22-MeV protons and at 7.5 MeV for the lower energies.

Selection of the Data

There exist many experimental results on the elastic scattering of protons by nuclei. Although we wanted to cover as large a range of A as possible, we have neglected the data for $Z<13$ because for lighter nuclei fluctuations in the parameters are expected to be larger due to nuclear structure differences and to the lower density of levels in the compound system. It was thought preferable at any one energy to study only the elements used in the same experiment. Then the values of the parameters may all be similarly affected by unsuspected systematic errors, and this would not obscure the existence of any trends as a function of A.

The neutron nonlocal optical analysis had shown that below an incident energy of 4 MeV, there were large contributions from compound elastic scattering. In the case of protons, the Coulomb barrier inhibits proton decay to excited states so that it seems preferable to be at least 4 MeV above the (p,n) threshold to avoid corrections for compound elastic scattering. Therefore, for most elements, the data below about 9 MeV are expected to be contaminated by compound elastic scattering. The lowest energy data used are then at 9.4 MeV from Greenlees *et al.*[19] The next large survey is by Dayton and Schrank[10] at 17 MeV. In order to close the gap between those two energies, the results for the medium-weight elements of Hu *et al.*[20] at 12 and 14.3 MeV were used. The recent results of Fulmer[21] at 22.2 MeV were also used. Because of the lower energy resolution of these later data, and since there was enough structure in the angular distributions for angles less than 120°, we ignored the data taken at wider angles where inelastic scattering contamination would be more important.

For all the data, the numerical values of the cross sections, as well as the estimated errors, were available. Mostly the relative errors are given as well as an estimate of the absolute errors. However, in order to avoid renormalization of the data, errors of 10% were assigned to all the data points except at 17 MeV where they were taken to be 5%. It is certain that some of the

[19] G. W. Greenlees, L. G. Kuo, and M. Petravic, Proc. Roy. Soc. (London) **A243**, 206 (1957).
[20] C. Hu, K. Kikuchi, S. Kobayashi, K. Matsuda, Y. Nagahara, Y. Oda, N. Takano, M. Takeda, and T. Yamazaki, J. Phys. Soc. Japan **14**, 861 (1959).
[21] C. B. Fulmer, Phys. Rev. **125**, 631 (1962).

results in this analysis are dependent upon this choice of uniform weighting for all angles. During the study, considerable difficulty was experienced with the 22.2-MeV data for Nb, Ta, and Au until these data were renormalized by 0.77, 1.39, and 1.28, respectively. Preliminary results by Fulmer[22] on the redetermination of the absolute magnitude of the cross section for these elements indicate approximate agreement with the renormalization for Nb and Ta.

Polarization data are now available in the energy region studied, but usually the results are not at energies, and on elements where the elastic differential cross section is also available. We have the same situation for the reaction cross sections. It was, therefore, decided not to include the polarization and the reaction cross-section data in the systematic analysis, but rather to compare them with the calculated results afterwards to see if they are consistent with the results based solely on the differential cross section.

III. RESULTS

For the results reported in this section, all the geometrical parameters have been kept fixed to the values given in Table V. The spin-orbit potential strength, V_{S0}, is fixed at 7.5 MeV for all elements except at 17 and 22.2 MeV where it is 8.5 MeV. Also, $W_S=0$.

In Table VI the results of the automatic search on V_S and W_D are given for the 35 elements. Two entries are found for Rh and Ag at 17 MeV. For the first one, as for all the other data, all the experimental points were used and the search code ended with a misfit of the angular distribution (visually, the experimental and theoretical curves are slightly out of phase). For the second one, the last five experimental points were neglected during the search and the experimental curve is well fitted up to 140°, but the fit is worse at backward angles. If the χ^2 for the experimental points which were neglected are added to the χ^2 in the second case, the new value of χ^2 thus obtained is, of course, larger than in the first case, but as judged visually the fit is better (to the author's eye).

The real well depth, V_S, at each energy increases with mass number. Following the suggestion of Bjorklund *et al.*,[23] the well depths, V_S, are plotted as a function of $Z/A^{1/3}$ in Fig. 4. The slope of the line drawn through the points at each energy increases slightly from 0.9 to 1.18 in going from 9.4 to 22.2 MeV. The intercepts with the $Z=0$ axis are plotted as a function of energy in Fig. 5.

TABLE V. Value of the geometrical parameters of the potentials kept fixed for all the investigation of Sec. III. All lengths are in fermi units. The spin-orbit potential strength V_{S0} is also kept fixed at 7.5 MeV for all the data below 17 MeV and at 8.5 MeV for the data at 17 and 22 MeV.

r_{0S}	a_S	r_{0I}	a_I
1.25	0.65	1.25	0.47

TABLE VI. Results of parameter search on V_S and W_D. $W_S=0$ and the other parameters are kept fixed to the values given in Table V.

Energy (MeV)	Element	V_S (MeV)	W_D (MeV)	σ_R (mb)	χ^2
9.4	Al	50.7	6.33	679	4.95
	Ni	51.4	16.4	769	4.87
	Cu	53.6	14.3	785	4.70
	Zn	53.8	13.4	768	0.63
	Ag	52.9	14.7	542	0.26
	Au	59.0	4.1	153	0.23
12.0	Ti	49.4	11.5	897	1.73
	Cr	50.8	12.7	909	5.00
	Ni	50.9	9.2	836	14.5
	Zn	51.9	13.3	916	3.09
14.3	Ti	48.7	13.0	966	2.65
	Cr	49.8	13.3	979	70.2
	Fe	49.4	13.8	981	5.40
	Ni	49.4	12.2	957	14.5
	Zn	50.0	14.0	998	4.16
17.0	Fe	47.9	11.5	1006	2.23
	Co	48.4	11.9	1020	6.40
	Ni	47.7	10.4	979	3.60
	Cu	48.5	10.9	1008	4.47
	Zn	48.5	12.4	1036	13.8
	Rh	53.3	16.1	1135	45.4
	Ag	52.7	14.9	1119	27.1
	Pt	53.8	18.7	1005	1.50
	Au	54.0	16.3	985	1.76
	Rh	50.6	16.0	1132	13.8
	Ag	50.9	15.0	1115	8.12
22.2	Al	43.4	9.0	758	2.00
	V	45.2	11.9	1029	2.00
	Mn	46.4	12.4	1062	1.64
	Co	46.5	11.6	1066	1.24
	Ni^{64}	46.2	12.0	1110	2.53
	Zn^{64}	46.1	13.7	1111	3.53
	Nb	49.5	13.1	1203	1.11
	Cd^{116}	50.1	15.6	1314	1.33
	Sn^{116}	50.8	13.9	1265	5.48
	Ta	53.9	17.9	1368	8.93
	Au	53.9	15.9	1333	3.91

One systematic feature which is observed for the fits at 9.4 and 12 MeV is that the first minima in the theoretical curves occur at slightly too small angles, but the second minima are at the right place. If one decreases slightly the well depths at these two energies, the first minima will be at the correct angles but the second minima will be fitted less well. If for the elements at 9.4 and 12 MeV we insist on fitting better the first minima, then the results obtained so far can be expressed by the relationship,

$$V_S=46.7-0.32E+Z/A^{1/3}. \quad (1)$$

This formula is very closely the same as the one implied by Bjorklund *et al.*[23]

A number of authors[24] have considered the possibility that the real part of the optical potential depends on the symmetry number $(N-Z)/A$. Lane [25] recently has

[22] C. B. Fulmer (private communication).
[23] F. Bjorklund, G. Campbell, and S. Fernbach, Suppl. Helv. Phys. Acta **6**, 432 (1961).
[24] J. Benveniste, R. Booth, and A. Mitchell, Phys. Rev. **133**, 1818 (1961). (This paper contains many references on this point.)
[25] A. M. Lane, Nucl. Phys. **35**, 676 (1962).

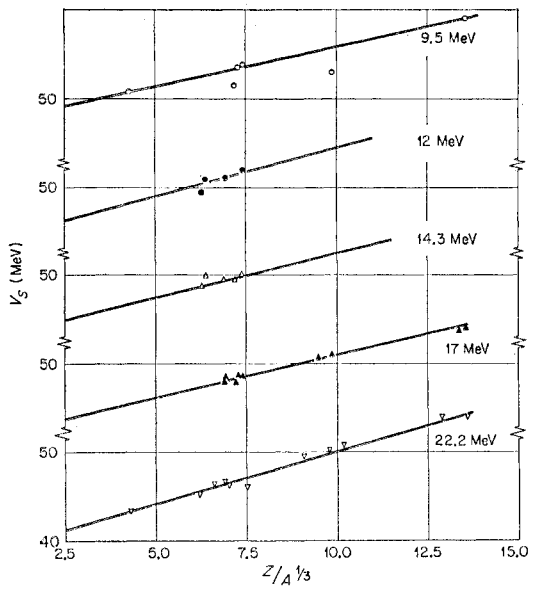

FIG. 4. Plot of the real well depths as a function of the Coulomb parameter $Z/A^{1/3}$. The geometrical parameters were kept fixed, for all the data, at the values given in Table V. The real potential and surface imaginary potential well depths were varied until a minimum value of χ^2 was obtained in each case. The numerical values of the well depths are given in Table VI.

investigated the isobaric spin dependence of the optical potential and shown that it gives rise to such a term. But before one can plot the well depth V_S as a function of $(N-Z)/A$, one must first subtract from it a variation with A arising out of the variation of the Coulomb potential[26] with Z. It is well known that the optical potential is expected to be momentum-dependent (or nonlocal). For example, let,

$$V_N = -V_{0N} + \alpha T,$$

where V_N is the specifically nuclear potential and T the kinetic energy of the incident particle inside the nucleus. Such a linear approximation for the dependence on T can be interpreted by an effective mass, and this relationship should be approximately valid over the small range of momenta considered. The kinetic energy is given by

$$T = E - V_N - V_c,$$

where E is the energy of the incident particle and V_c the Coulomb potential. We have then,

$$V_N = -\frac{V_{0N}}{1+\alpha} + \frac{\alpha}{1+\alpha}E - \frac{\alpha}{\alpha+1}V_c.$$

Then the nuclear part of the potential, V_N, should vary as a function of V_c in the same manner as for the incident energy E. It is known from the neutron analysis that the coefficient of E is approximately 0.3. It is then expected to have the nuclear potential increase as $0.3V_c$ solely from the momentum dependence of the potential. The Coulomb potential does not have the same radial dependence as the nuclear potential. It was decided, therefore, to apply the above correction to the well depth by using an average value of the Coulomb potential inside the nucleus. For a uniformly charged sphere of radius $1.25A^{1/3}$F, this is

$$\bar{V}_c = (1.38Z/A^{1/3}) \text{ MeV}.$$

Then the correction is taken to be

$$0.3\bar{V}_c = (0.4Z/A^{1/3}) \text{ MeV}.$$

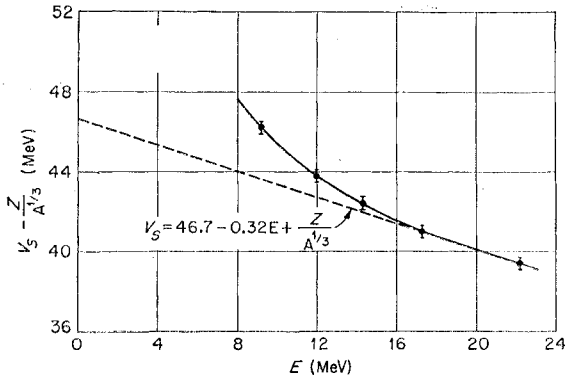

FIG. 5. Intercepts of the lines of Fig. 4 with the axis $Z=0$ as a function of bombarding energy. The formula gives an approximate value of the real well depth as a function of energy and the Coulomb parameter $Z/A^{1/3}$.

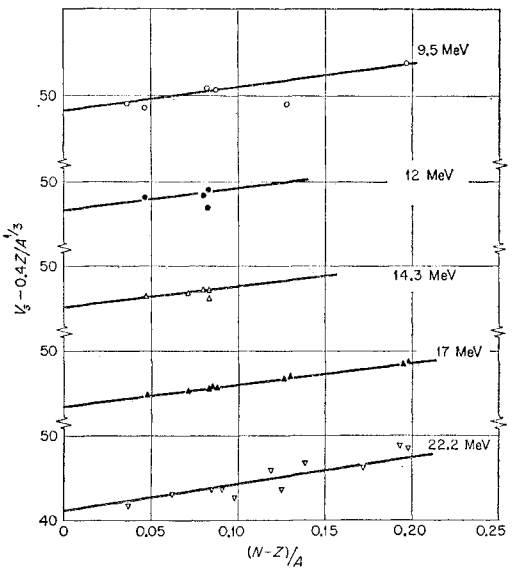

FIG. 6. Plot of the real well depths, corrected for the Coulomb potential variation $(-0.4Z/A^{1/3})$, as a function of the symmetry parameter $(N-Z)/A$. The well depths are the same as those in Fig. 4 and their numerical values are given in Table VI. The slope of the lines, 27 MeV, gives the coefficient of the symmetry term in the optical potential.

[26] A. M. Lane, Rev. Mod. Phys. **29**, 191 (1957).

In Fig. 6 the well depth, V_S, corrected for the Coulomb potential dependence, $(V_S-0.4Z/A^{1/3})$, is plotted as a function of $(N-Z)/A$ for all the nuclei. Comparison with Fig. 4 shows that the linear correlation is about the same for the three lowest energies and at 17 MeV it is slightly improved, but at 22.2 MeV slightly worse. Since the correlation was best at 17 MeV, this energy was used to determine the slope, 27 MeV while at the other energies the same slope was used.

In order to verify that there was not a great loss of fit by assuming the linear dependence in Fig. 4, the well depths were read from the lines and the search code readjusted W_D for a lowest χ^2 with these values of V_S. The results are given in Table VII and the curves are shown in Figs. 7, 8, and 9. Comparison with the χ^2 in Tables VI and VII shows that, in general, the fits have not worsened very much. In fact, the general nature of the fits in Figs. 7, 8, and 9 is very similar to what had been obtained from the parameters of Table VI. In Fig. 7 at 9.4 and 12 MeV for most cases the first minimum is at too small angles but the second minimum is usually well located. In Fig. 8 for the medium-weight elements the first minima are properly given, but with the exception of Fe all the theoretical curves are too high in the region of 40°. For Rh and Ag the fit at angles greater then 140° is unsatisfactory. Almost all the elements in Fig. 9 are not fitted well at angles greater than 140°, but it should be remembered that data only up to 120° were used in the search. The disagreement for Ta and Au also starts at much smaller angles—about 100°. The inclusion of some volume imaginary potential will be found later to improve the fits at backward angles for these 22.2-MeV data.

In Fig. 10 the intercepts of the lines of Fig. 6 with the axis $(N-Z)/A=0$ are plotted as a function of energy. We have then, combining the results of Figs. 6 and 10,

$$V_S=53.3-0.55E+\left[0.4\frac{Z}{A^{1/3}}+27\frac{(N-Z)}{A}\right]. \quad (2)$$

The fact that both $Z/A^{1/3}$ and $(N-Z)/A$ for stable nuclei increase in similar fashion through the periodic table, together with the fact that there are fluctuations in the well depth, prevents a clear-cut separation of the A dependence into the part due to the change in Coulomb potential and the symmetry term. This point, as well as the reason for selecting $-0.3E$ as the energy dependence when evaluating the Coulomb potential effect, will be discussed in the next section.

Since a systematic trend had been found for the real well depth V_S and the imaginary potential was still allowed to vary, a_I was increased to 0.65F for all the elements and the code allowed to readjust W_D. It was found that, in general, the new fits were unchanged or worse with the exception of Cu at 9.47 MeV, Rh, Ag, and Au at 17 MeV, and Sn, Ta, and Au at 22.2 MeV. The new fits are given by the dashed lines on Figs. 8 and 9. The effect of a larger a_I is to give a larger σ_R, for instance, on Cu at 9.47 MeV it increased to 867 mb. With the exception of Cu at 9.47 MeV, it may be significant that only the fits to heavier nuclei have been improved by making the surface-imaginary potential wider.

TABLE VII. Values of the parameter W_D, readjusted by the code when the real well depths V_S are fixed to the values given by the lines of Fig. 6. All the other parameters are as given in Table V. The elastic angular distributions corresponding to those parameters are compared to the data on Figs. 7, 8, and 9.

Energy (MeV)	Element	V_S (MeV)	W_D (MeV)	σ_R (mb)	χ^2
9.4	Al	50.9	6.35	679	4.94
	Ni	52.3	15.8	769	5.00
	Cu	53.5	14.3	785	4.75
	Zn	53.4	13.4	765	0.74
	Ag	55.6	14.4	534	0.85
	Au	58.8	5.0	149	0.60
12.0	Ti	51.3	13.1	922	13.4
	Cr	51.3	12.8	911	5.78
	Ni	50.7	9.4	838	14.5
	Zn	51.8	13.3	915	3.17
14.3	Ti	49.9	13.6	975	6.95
	Cr	50.0	13.4	981	70.5
	Fe	49.8	14.0	982	5.79
	Ni	49.4	12.2	956	14.5
	Zn	50.5	13.4	994	4.58
17.0	Fe	48.0	11.5	1005	2.23
	Co	48.4	11.8	1020	6.40
	Ni	47.7	10.4	979	3.60
	Cu	48.7	10.9	1008	4.49
	Zn	48.7	12.4	1036	13.9
	Rh	50.6	16.2	1127	81.8
	Ag	50.9	15.6	1120	49.6
	Pt	54.0	19.2	1007	1.62
	Au	54.1	16.4	986	1.76
22.2	Al	43.5	9.02	758	2.00
	V	46.0	12.0	1032	2.31
	Mn	45.9	12.4	1060	1.73
	Co	46.0	11.6	1064	1.35
	Ni^{64}	47.1	12.2	1139	3.11
	Zn^{64}	45.5	13.7	1110	3.84
	Nb	47.7	13.6	1209	3.40
	Cd^{116}	49.5	15.7	1314	1.58
	Sn^{116}	48.7	14.5	1267	10.0
	Ta	51.4	17.4	1352	10.0
	Au	51.7	15.7	1325	5.55

Various correlations were tried for the W_D of Table VII, but due to the large fluctuations for adjacent nuclei, evidence for none of them was found to be very strong. The only evident trend is that W_D increases as one goes from lighter to heavier nuclei. There is no evidence for a systematic increase of W_D as one goes to higher energy—in fact, the trend may be for a slight decrease in W_D. Since the form of the imaginary potential is an extreme one (all in the surface), one cannot draw strong conclusions about the variations of W_D before investigating the effect of adding some volume imaginary potential, as discussed in the next section. However, to summarize the results with pure surface imaginary potential, one may say that below 17 MeV for the medium-weight elements $W_D=13.5\pm2.0$ MeV. At 17 and 22.2 MeV we may express the increase of W_D

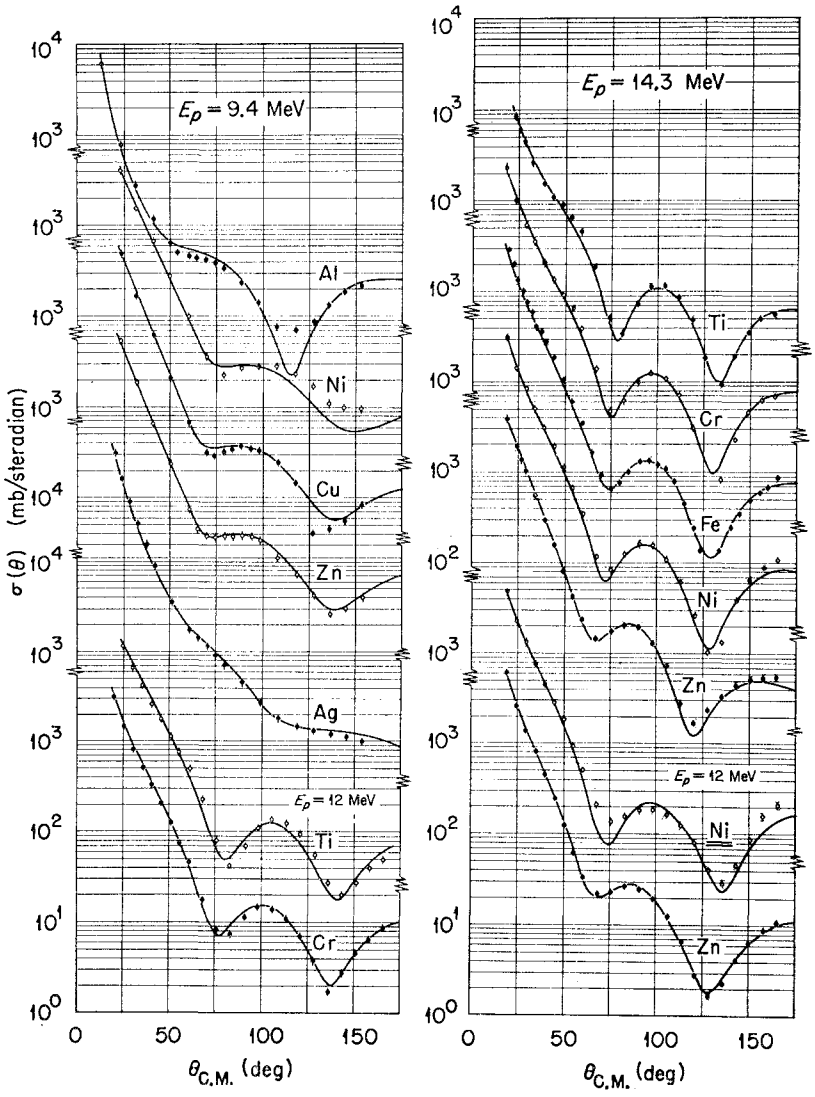

FIG. 7. Comparison of the optical-model calculations with the 9.4-, 12-, and 14.3-MeV data. The geometrical parameters of the potentials are fixed in all cases to the values given in Table V. The real well depth was read off the appropriate curve in Fig. 6. The imaginary potential well depth was the only parameter adjusted for a minimum value of χ^2 in each case. The real and imaginary potential well depths corresponding to the curves are given in Table VII.

as we go to heavier nuclei by

$$W_D = 3A^{1/3} \pm 1.5 \text{ MeV},$$

as one can see from Fig. 11 where W_D is plotted as a function of $A^{1/3}$. A somewhat better correlation is actually found from a plot of W_D versus $(N-Z)/A$ as shown on Fig. 12. The appropriate formula for W_D is given on the figure at each energy.

Let us now compare the experimental reaction cross sections and elastic-scattering polarizations with the values obtained from the parameters of Table VII (or calculated using the above formulas for V_S and W_D when the correspondlng elastic-scattering angular distributions are not available). On Fig. 13 are shown some of the results for the elastic polarization.[18,27,28] The theoretical curves were obtained from the parameters of Table VII at the nearest energy. In general, the agreement is good but for the two lower energies there are large disagreement at angles greater than 140°. Rosen[29] finds that at 14.5 MeV the polarization up to about 120° varies smoothly with elements but that at larger it varies very rapidly from element to element and for different isotopes. It is not clear that this new data can be fitted at large angles with only small deviations from the parameters of the present analysis.

In Table VIII is given the comparison of the measured reaction cross section with the calculations. The 10-MeV data is from Wilkins and Igo[17]; when there is a second entry for the same element it is the result of Albert and Hansen[14] at 9.85 MeV. Both sets of numbers have been read off from published graphs. The cal-

[27] L. Rosen and W. T. Leland, Phys. Rev. Letters 8, 379 (1962).
[28] W. S. Blanpied, Phys. Rev. 113, 1099 (1959).
[29] L. Rosen (private communication).

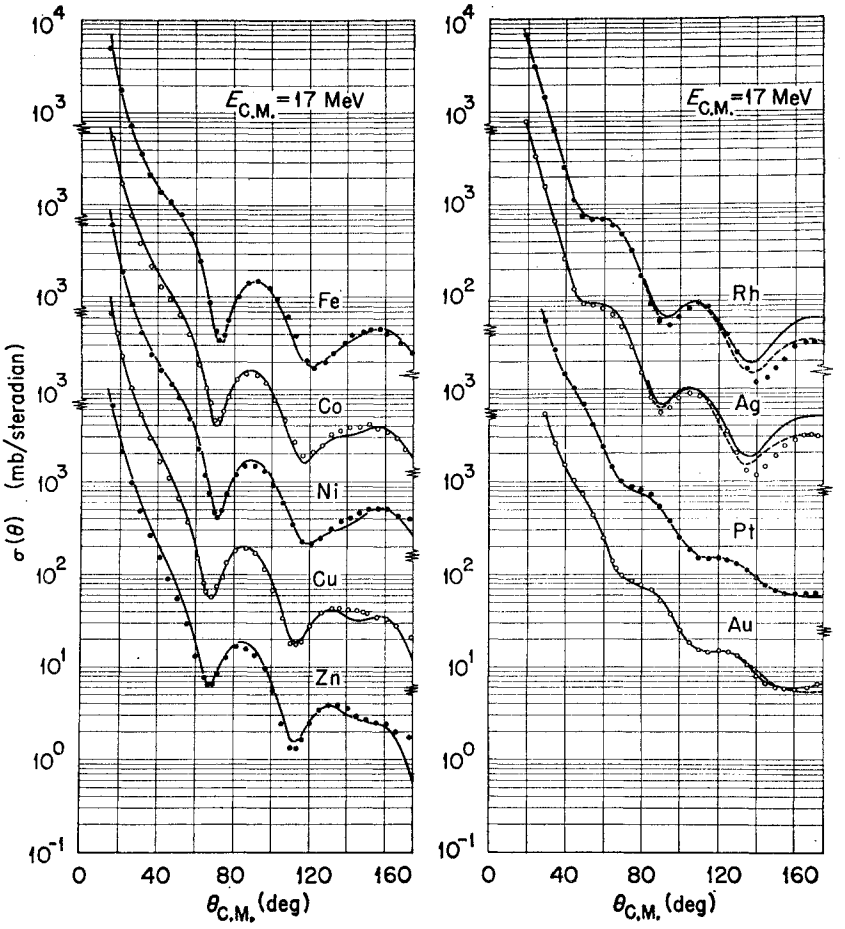

FIG. 8. Comparison of the optical-model calculations with the 17-MeV data. The geometrical parameters of the potentials are fixed in all cases to the values given in Table V. The real well depth was read off the appropriate curve in Fig. 6. The imaginary potential well depth was the only parameter adjusted for a minimum value of χ^2 in each case. The real and imaginary potential well depths corresponding to the curves are given in Table VII. The dashed curves for Rh, Ag, and Au are the results when the diffuseness parameter a_I is set to 0.65 F instead of the value 0.47 F for the full curves.

culations were done at 10 MeV using formula (2) to calculate V_S and the imaginary potential from the relation $W_D=3.5A^{1/3}$ MeV. The 17-MeV data are due to Pollock[30] and the 22.2-MeV data is Fulmer's.[31] In general, there is agreement with the measured cross section, but this is not too surprising since the 10-MeV data were known to be in agreement with Bjorklund's calculation and our parameters are very similar. It may be significant that at 10 MeV for the light nuclei the calculated cross sections are slightly too high.

IV. DISCUSSION

Effects of Core Excitations

In the usual optical-model treatment of elastic scattering, as in this paper, one takes care of the nonelastic channels by the introduction of an imaginary part to the potential. In many even-even nuclei, the first 2^+ excited state, which can be interpreted as due to collective nuclear motions, is strongly excited by inelastic scattering of medium-energy protons. One may then expect that the excitation of this state could affect the elastic scattering in a way which cannot be easily represented by a central complex potential. In slow neutron scattering it has been shown[32] that the virtual excitation of those states changes appreciably the strength functions. Buck[33] recently has extended the formalism to include the consideration of charged incident particles, spin-orbit effects, and easy specialization to rotational and vibrational model. This is done by setting up and solving a system of coupled equations. It is found that for most coupling strengths required to fit the inelastic-scattering cross sections, the elastic-scattering cross sections are appreciably different from the weak-coupling limits. The interchannel coupling strength is proportional to a deformation parameter β. In the energy range covered by this analysis, Buck has found that β corresponded very closely to the deformation parameter obtained from Coulomb excitation of the 2^+ state and is related to the $B(E2)$ in the following

[30] R. E. Pollock (private communication).
[31] C. B. Fulmer, Phys. Rev. **116**, 418 (1959).
[32] B. Margolis and E. S. Troubetzkoy, Phys. Rev. **106**, 105 (1957); D. M. Chase, L. Wilets, and A. R. Edmonds, *ibid.* **110**, 1080 (1958); B. Buck and F. Perey, Phys. Rev. Letters **8**, 444 (1962).
[33] B. Buck, Phys. Rev. **130**, 712 (1963).

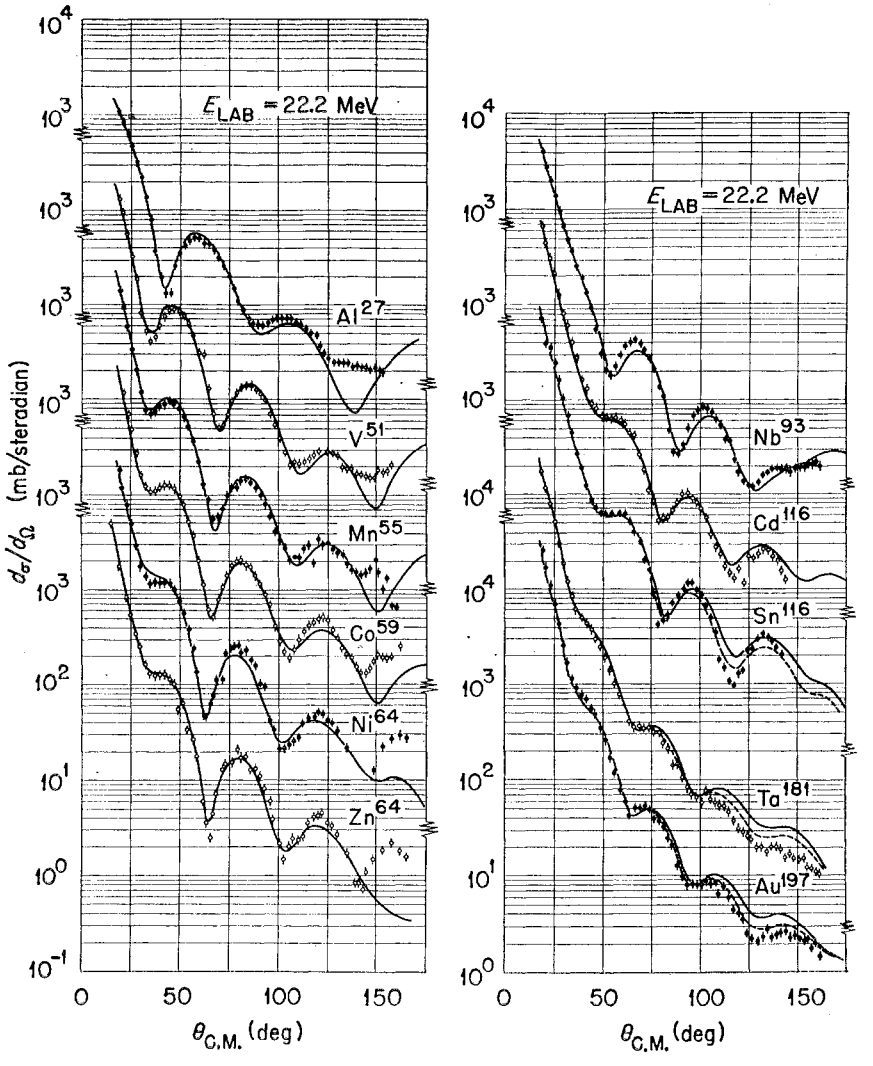

FIG. 9. Comparison of the optical-model calculations with the 22.2-MeV data. The geometrical parameters of the potentials are fixed in all cases to the values given in Table V. The real well depth was read off the appropriate curve in Fig. 6. The imaginary potential was the only parameter adjusted for a minimum value of χ^2 in each case. The real and imaginary potential well depths corresponding to the curves are given in Table VII. The dashed curves for Sn, Ta, and Au are the results when the diffuseness parameter a_I is set to 0.65 F instead of the value 0.47 F for the full curves.

fashion:

$$\beta^2=\frac{B(E2:0\rightarrow 2)}{[(3/4\pi)ZeR_c^2]^2},$$

where R_c is the radius of the charge distribution. From Coulomb excitation it is known that the β's vary appreciably, from 0.1 to above 0.4. However, for most

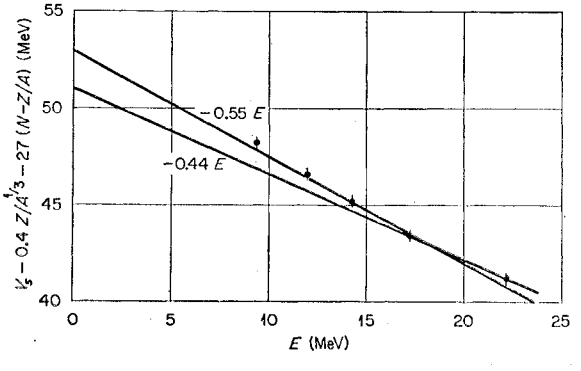

FIG. 10. Intercepts of the lines of Fig. 6 with the axis $(N-Z)/A=0$ as a function of energy.

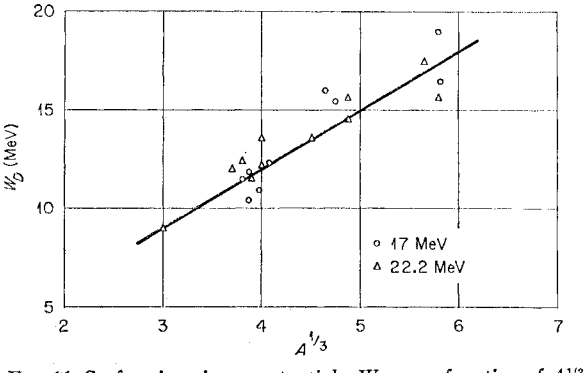

FIG. 11. Surface imaginary potentials, W_D, as a function of $A^{1/3}$ for the fits to the 17- and 22.2-MeV data. The curves corresponding to those values of W_D are given in Figs. 8 and 9. The numerical values are given in Table VII.

nuclei studied, β is between 0.2 and 0.3. Buck has illustrated in his paper the effect of varying the coupling strength for Ti at 14.5 MeV. In Fig. 14 is shown the effect of varying β for Fe^{56} at 17 MeV. As β increases, the diffraction curve at backward angles is displaced toward smaller angles, but the position of the first minimum is not appreciably affected. If one tries to fit such a curve out to 180° with the ordinary optical model, one has to compromise on the position of the minima. As β increases, the well depth V_S must increase to move the diffraction pattern at backward angles, with the result that the ordinary optical-model curve has its first minimum at too small angles. It seems that at 9.4 and 12 MeV the fits to the data which we have obtained show this effect.

In order to obtain quantitative estimates of the effect of strong coupling on the ordinary optical-model parameters a series of calculations were performed. With the following parameters,

$$V_S = 52.2 - 0.3E \text{ MeV}, \quad W_D = 11.5 \text{ MeV},$$
$$r_{0S} = 1.25 \text{ F}, \quad r_{0I} = 1.25 \text{ F},$$
$$a_S = 0.65 \text{ F}, \quad a_I = 0.47 \text{ F},$$
$$V_{S0} = 7.5 \text{ MeV},$$

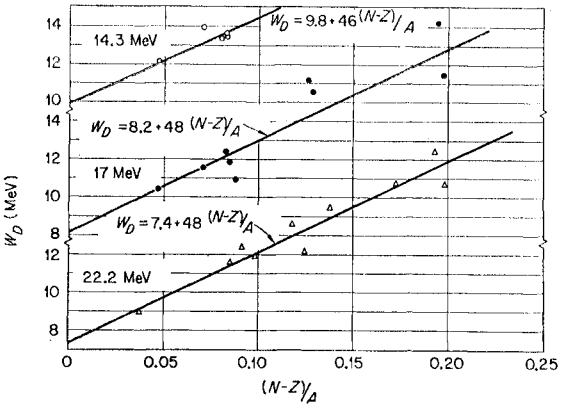

FIG. 12. Surface imaginary potentials, W_D as a function of the symmetry parameter $(N-Z)/A$ for the fits to the 14.3-, 17-, and 22.2-MeV data. The curves corresponding to those parameters are given in Figs. 7, 8, and 9 and the numerical values in Table VII.

the coupled-channel code was run for Fe^{56}, with the energy of the 2^+ state at 0.85 MeV, at incident proton energies of 10, 12, 14, 17, and 22 MeV. The parameter β was also varied from 0.1 to 0.4. Using those theoretical curves as "data" the search code was run with the

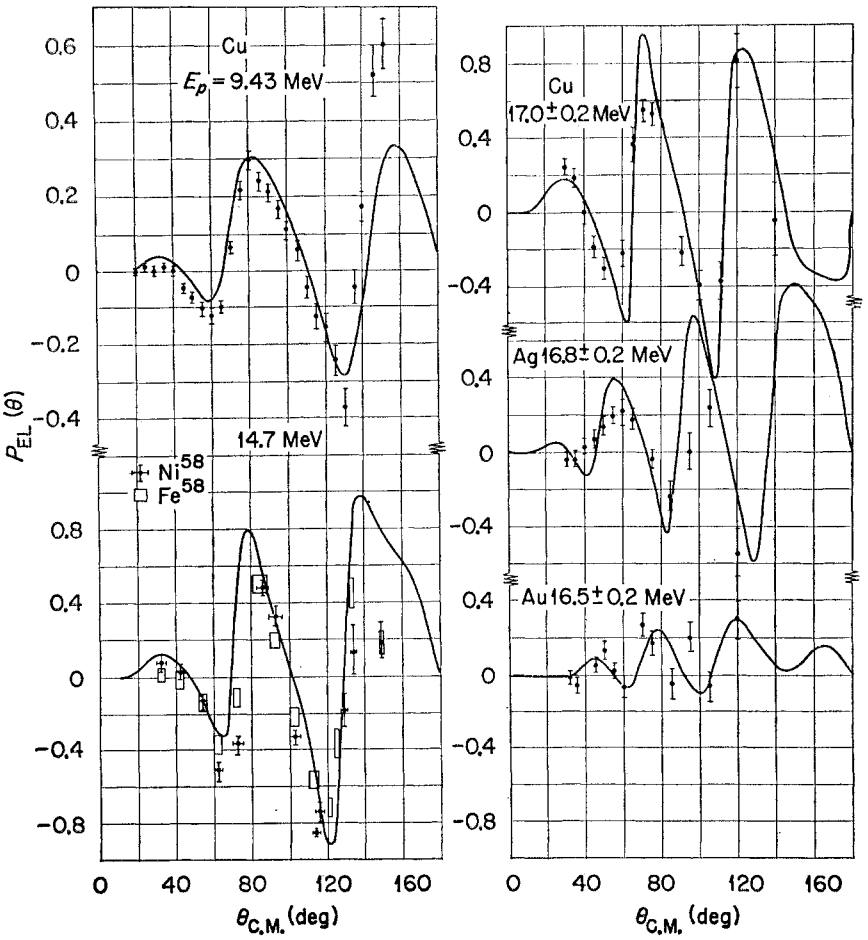

FIG. 13. Comparison of the elastic polarization data with the predictions from the analysis based only on the elastic differential cross section. The curves correspond to the calculations given in Figs. 7 and 8 for the elastic differential cross sections.

TABLE VIII. Comparison of theoretical and experimental reaction cross sections. At 10 MeV the first entries are the data of Wilkins and Igo (Ref. 17), and the second are those of Albert and Hansen (Ref. 14). The data at 17 MeV are from Pollock (Ref. 30) and at 22 MeV from Fulmer (Ref. 31).

Energy (MeV)	Element	σ_R Experimental (mb)	σ_R Theoretical (mb)
10	Al	705^{+25}_{-10}	
		780^{+61}_{-43}	799
	Sc	800±40	853
	Ti	768±40	855
		850±40	
	Mn	753±40	848
	Ni	702±40	793
		730±40	
	Cu	816±40	832
		850±40	
	Zn	840±40	817
	Y	792±70	761
	Zr	710±70	743
	Mo	770±70	708
	Rh	730±70	652
		620±40	
	Ag	690±50	616
		620±40	
	Sn	720±70	589
		640±40	
	Ta	280±100	227
		240±20	
	Au	180±150	160
		160±20	
17	Al	712±36	789
	Ni	886±55	979
	Cu	968±66	1008
	Pb	1330±180	1050
22	U	1400±100	1325

ordinary optical model and the well depths V_S and W_D adjusted until a minimum value of χ^2 was obtained. The geometrical parameters and the spin-orbit potential strength were kept to the same value as in the coupled channel calculation. The results for V_S are plotted in Fig. 15, where it is seen that the energy variation of the real well depth depends very sensitively on the coupling parameter β. It is also found that W_D depends very much on β and that the effect is bigger the lower the energy. To a very good approximation the increase in V_S and W_D is a linear function of β^2 for the cases considered,

$$\Delta V_S = C_1\beta^2, \tag{3a}$$

$$\Delta W_D = C_2\beta^2. \tag{3b}$$

TABLE IX. Variation as a function of energy of the coefficients c_1 and c_2 of Formulas 3.

Energy (MeV)	c_1 (MeV)	c_2 (MeV)
10	32	45
12	28	25
14	23	25
17	18	25
22	8	18

The coefficients C_1 and C_2, which are energy-dependent are given in Table IX. C_1 shows a smooth energy dependence but it is not clear why C_2 has the same value at the 3 intermediate energies. The coefficients C_1 and C_2 are probably functions of the size of the nucleus and to a lesser degree of the energy of the 2^+ excited state. However, the values we have thus obtained should be representative of the nuclei in this mass region. To illustrate that this effect is noticed in the elements studied, in Fig. 16 the real well depths are plotted as a function of energy for the neighboring nuclei Ni and Zn which are characterized by values of β of 0.20 and 0.25, respectively, for the most abundant isotopes. The

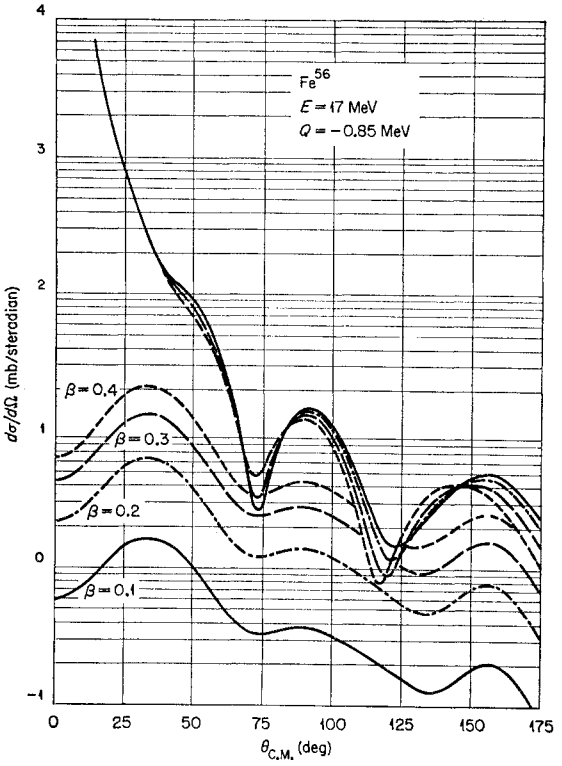

FIG. 14. Effect of the variation of the coupling parameter β on the elastic and inelastic differential cross sections for Fe at 17 MeV.

energy dependence of $-0.43E$ for Ni and $-0.62E$ for Zn is significantly different. It is also seen in Table VII that, except at 9.4 MeV where compound elastic scattering is important in Ni, the imaginary potential is much smaller for Ni at all energies. Some of the observed difference between the parameters for Ni and Zn certainly comes from the different coupling of their respective 2^+ collective states.

Many of the angular distributions analyzed in this paper were obtained from even-odd or odd-even targets. It is probable that the arguments concerning the effects of the strong coupling of the quadrupole collective state in even-even nuclei are still valid. Indeed, strong quad-

rupole inelastic scattering is observed in odd nuclei,[34] although the strength of the single transition found in even nuclei is shared by several excited states in the odd nuclei. Arguments have been presented that the effects on the elastic scattering of virtual excitation of these states is very similar to that in the even nuclei.[35]

The results of Buck's analysis differ from ours; however, the differences can now be understood in terms of our neglect of the strongly coupled 2^+ channel. In both analyses the 3^- collective state, which is also known to be strongly excited, has been neglected. It is probable that its effect will be similar to that of the 2^+ level.

Nuclear Symmetry Term

It follows that the strong energy dependence of the real well depth in formula (2) is partly due to the neglect of core excitations and our insistance on fitting the angular distribution to large angles. The results of the neutron analysis and of Buck give the weaker energy

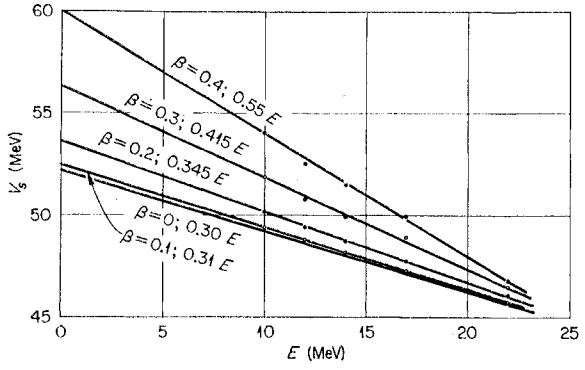

FIG. 15. Equivalent spherical optical potential well depths as a function of energy, for various value of the coupling strength β, in Fe.

dependence of $-0.3E$. It is for this reason that $0.3E$ was used to correct for the change in well depth due to the Coulomb potential variation as a function of Z. It has already been pointed out that both the symmetry number $(N-Z)/A$ and the Coulomb parameter $Z/A^{1/3}$ vary very similarly as a function of mass number for stable nuclei. Because of fluctuations in the well depth V_S it is not possible to extract unambiguously its dependence on $Z/A^{1/3}$ or $(N-Z)/A$ separately and, therefore, one of the two dependences must be subtracted out first to find the other one. We thought that the momentum correction due to the Coulomb potential was more easily justified, although some ambiguities still remain due to the effect of the strong coupling on the energy dependence. In principle, the ambiguity could be resolved by the study of the neutron optical potential, for which the symmetry term has the opposite sign and

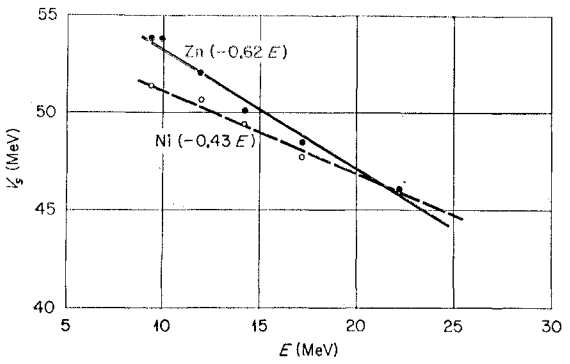

FIG. 16. Real well depth, V_S as a function of energy for Zn and Ni.

the Coulomb correction is absent. Unfortunately, the neutron data in the energy region of interest are sufficiently imprecise that generally it is not possible to determine the symmetry dependence unambiguously.

In view of the fluctuations in the potential depths, it seems preferable to take as many nuclei as possible at a given energy to determine the nuclear symmetry term, so that its mean value can be obtained and the strong coupling effects averaged over many values of β. Variations in the effect of strong coupling make difficult the determination of the nuclear symmetry term when the scattering from only 2 isotopes or isobars, at one energy, are compared (for instance, Ni^{64} and Zn^{64} have values of β of 0.19 and 0.25, respectively). For example, the 11-MeV data of Beurtey *et al.*[36] on the 3 isotopes of Zn show no nuclear symmetry effect when analyzed with the ordinary optical model, the increase in the well depth due to symmetry being compensated for by the effective decrease due to the variation of β in the 3 isotopes. When analyzed with the coupled-equations theory, the symmetry effect becomes more apparent, although smaller than the average value we have determined previously.

There is no strong reason to believe that the radial form factor for the nuclear symmetry part of the potential is of the same Saxon shape as the main part of the potential, as we have assumed. In fact, since it probably arises mainly from interaction with the excess neutrons, one might expect its shape to change as a function of mass number, as these neutrons fill new shells. It is also quite possible that some of the geometrical parameters, which we have kept fixed, vary in some systematic way as a function of A. In this case, the variation would have been compensated for, in our analysis, by adjusting V_S, so that it is included in the well-depth change due to the nuclear symmetry term which we observe. We have also neglected any energy variation which the symmetry term may have in the energy region studied here, but it would have to be large for us to see it.

[34] F. Perey, R. Silva, and G. R. Satchler, Phys. Letters 4, 26 (1963).
[35] G. R. Satchler (to be published).
[36] R. Beurtey, P. Catillon, R. Chaminade, H. Faraggi, A. Papineau, and J. Thirion, Nucl. Phys. 13, 397 (1959).

Hodgson[37] has analyzed the scattering of 96-MeV neutrons from various nuclei using for the real well the same geometrical parameters as Bjorklund. His results are then directly comparable to ours, and he finds[12]

$$V_S = 24 - 38[(N-Z)/A] \text{ MeV}.$$

This increase over our value may reflect an energy dependence of this term.

Drisko, Bassel, and Satchler,[38] analyzing the V^{51} (p,n) angular distribution leaving the residual nucleus in a state which is the isobaric analog of the target ground state, find that the value of the symmetry term obtained in this paper gives fairly good agreement with the magnitude and shape of the cross section. The other parameters in their analysis are also as given by this paper. Hodgson and Rook[39] analyzing the same data give an estimate of $35[(N-Z)/A]$; this is based purely on the peak cross section since they could not reproduce the shape of the cross section.

Another independent determination of the magnitude of this term in the shell model is obtained by Sood,[40] from an analysis of the well depth needed to give the nucleon separation energy in a range of nuclei. The value which he finds is $28.5[(N-Z)/A]$ MeV. It is interesting to note, from Sood's results, that in the bound-state case he does not find it necessary to correct the proton well depth for the Coulomb potential variation as we had to do in the scattering case. This may imply a different energy variation for the potential for the bound states and for the elastic scattering in the energy range we have studied here.

If one applies formula (2) to calculate the neutron potential well depth, using a value of $(N-Z)/A=0.1$ appropriate to medium-weight nuclei, the value of V_S is about 1.5 MeV from the values of Bjorklund and Fernbach,[2] being too high at 7 MeV but too low at 4.1 and 14.5 MeV. This seems to resolve the 10-MeV discrepancy[4] between the neutron and proton real well depth.

To summarize, there seems to be fairly strong evidence for the symmetry term in the optical model. Its magnitude is not well determined but is found, from detailed comparison of calculations with experiment, to be of the order of $(30\pm10)[(N-Z)/A]$ MeV. This is well within the original estimates of Lane.[25]

Volume Imaginary Potential

At this stage of the analysis some volume imaginary potential was added to the potential. The procedure adopted was to keep all the geometrical parameters the same as before and to grid on the value of W_S, allowing the search code to readjust V_S and W_D for a minimum χ^2 at each value of W_S. The results for the 3 lowest energies did not show any systematic trend as a function of W_S, but at 17 and 22 MeV some definite trends were found.

The addition of W_S, in general, leaves V_S unchanged but reduces the value of W_D by an amount approxi-

TABLE X. Values of the surface imaginary potential W_D as a function of volume imaginary potential, W_S. The numbers in parentheses are the corresponding values of χ^2. In Fig. 17 the curves for the values of $W_S=0$ and $W_S=3$ MeV are compared to the data at 17 MeV. For the values of $W_S=0$ and $W_S=5$ MeV a similar comparison was done for the 22.2-MeV data, as shown in Fig. 18.

Energy (MeV) \ W_S (MeV)	Element	0.	1.	2.	3.
17	Fe	11.5 (2.23)	10.1 (3.38)	8.9 (5.73)	7.8 (8.82)
	Co	11.9 (6.40)	10.4 (6.68)	9.1 (7.85)	7.9 (9.71)
	Ni	10.4 (3.60)	9.1 (4.88)	7.9 (6.80)	6.7 (9.17)
	Cu	10.9 (4.47)	9.5 (5.39)	8.3 (6.76)	7.1 (8.68)
	Zn	12.4 (13.8)	10.9 (11.7)	9.6 (10.0)	8.2 (9.08)
	Rh	16.1 (45.4)	14.5 (35.6)	12.9 (25.7)	11.0 (16.4)
	Ag	14.9 (27.1)	13.5 (21.1)	12.0 (15.2)	10.6 (10.1)
	Pt	18.7 (1.55)	17.9 (1.69)	17.1 (2.04)	16.5 (2.55)
	Au	16.3 (1.76)	15.4 (1.33)	14.5 (1.30)	13.7 (1.60)
W_S (MeV)		0.	2.	3.	5.
22.2	Al	9.0 (2.04)	7.3 (1.04)	6.4 (0.75)	4.9 (0.53)
	V	11.9 (2.04)	9.6 (1.33)	8.6 (1.28)	6.6 (1.84)
	Mn	12.4 (1.64)	10.0 (1.22)	8.9 (1.28)	6.8 (1.91)
	Co	11.6 (1.24)	9.3 (1.64)	8.2 (2.11)	6.2 (3.44)
	Ni	12.0 (2.53)	9.5 (2.64)	8.4 (3.04)	6.3 (4.38)
	Zn	13.7 (3.53)	10.8 (2.80)	9.5 (2.68)	7.1 (3.02)
	Nb	13.1 (1.11)	9.6 (1.58)	8.1 (2.04)	5.2 (3.46)
	Cd	15.6 (1.33)	13.0 (1.09)	12.0 (2.04)	11.1 (3.00)
	Sn	13.9 (5.48)	11.2 (4.02)	9.8 (3.97)	7.5 (5.00)
	Ta	17.9 (8.93)	14.5 (4.62)	13.1 (3.13)	11.0 (1.33)
	Au	15.9 (3.91)	12.8 (1.56)	11.5 (0.93)	9.7 (0.53)

[37] P. E. Hodgson, Nucl. Phys. **21**, 21 (1960).
[38] R. M. Drisko, R. H. Bassel, and G. R. Satchler, Phys. Letters **2**, 318 (1962).
[39] P. E. Hodgson and J. R. Rook, Nucl. Phys. **37**, 632 (1962).
[40] P. C. Sood, Nucl. Phys. **37**, 624 (1962).

mately equal to W_S. As W_S increases the elastic differential cross section is lowered in the region of the first minimum near 40°, otherwise the curve is almost unchanged up to about 125° where it starts to oscillate more. Table X contains the values of W_D and χ^2 as W_S is increased for the two higher energies.

At 17 MeV for the 4 lightest elements χ^2 increases as a function of W_S. Up to about $W_S=3$ MeV the fit at forward angles is improved but the oscillations are too large at backward angles. The case of Zn is very similar except that the improvement in the forward angles more than compensates for the loss of fit at backward angles. For Pt and Au the fits are not changed appreciably but for Rh and Ag the over-all fit is much improved. On Fig. 17 the curves are given for the two cases $W_S=3$ MeV and $W_S=0$.

At 22.2 MeV, it may be recalled that in the search only the angles up to 120° are used and the χ^2 only applies to those angles. On average as W_S increases the χ^2 decreases until it reaches a minimum value at about $W_S=3$ MeV and then increases to the point where at $W_S=5$ MeV the χ^2 is approximately the same as at $W_S=0$. The curves for $W_S=0$ and $W_S=5$ MeV are plotted on Fig. 18. With the exception of Nb the fits have much improved at back angles, particularly for Co, Ni, Zn, Ta, and Au. Around the first minimum the experimental points lie between the curves for the extreme values of $W_S=0$ and $W_S=5$ MeV; for most elements the best agreement in this region of angles is for $W_S=3$ MeV.

For all the elements at 17 and 22.2 MeV, the effect of adding a volume term to the imaginary potential has been to raise the reaction cross section by from 3 to 4%. Therefore, the comparison with the experimental values of σ_R does not guide us to prefer some volume absorption.

One can conclude that at 17 MeV there is at most 3 MeV of volume imaginary potential and at 22.2 MeV this limit has increased to about 5 MeV. At lower energies the variations of the fits are not systematic enough to obtain an estimate of the amount of volume imaginary potential. In the range of energy studied the

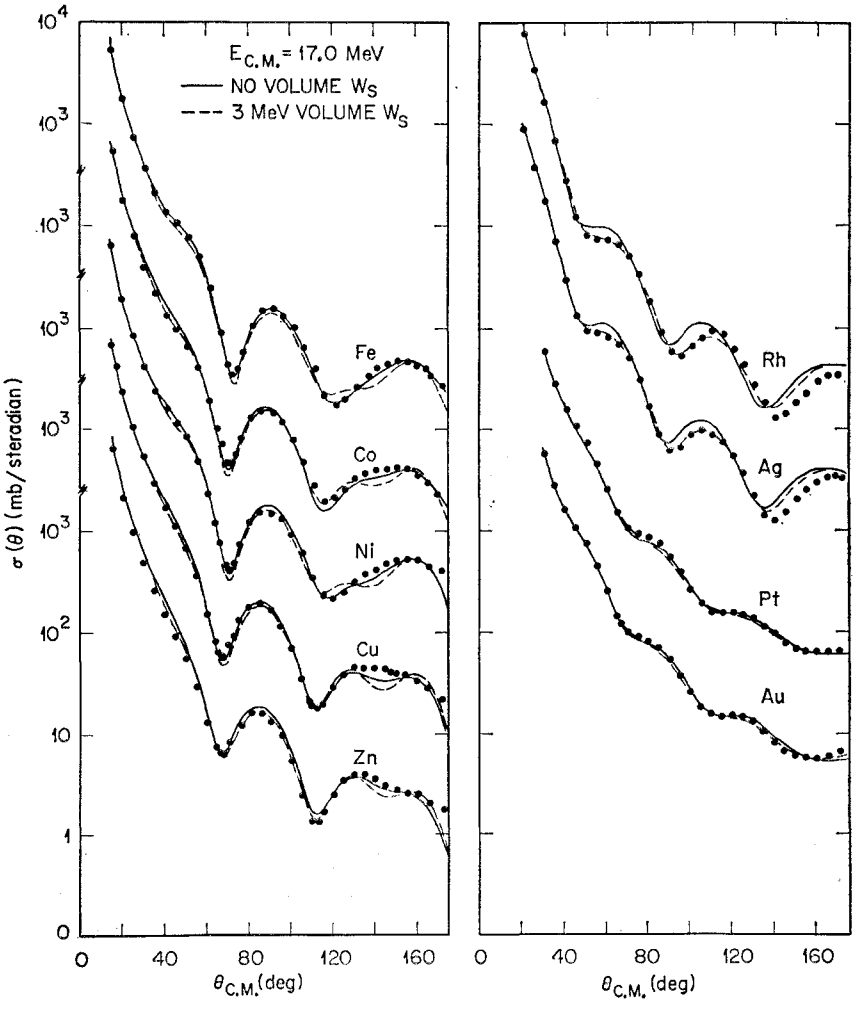

FIG. 17. Effect of volume imaginary potential on the fits to the 17-MeV data. The geometrical parameters are kept fixed at the values of Table V, the well depths, V_S and W_D are adjusted for lowest χ^2 in each case.

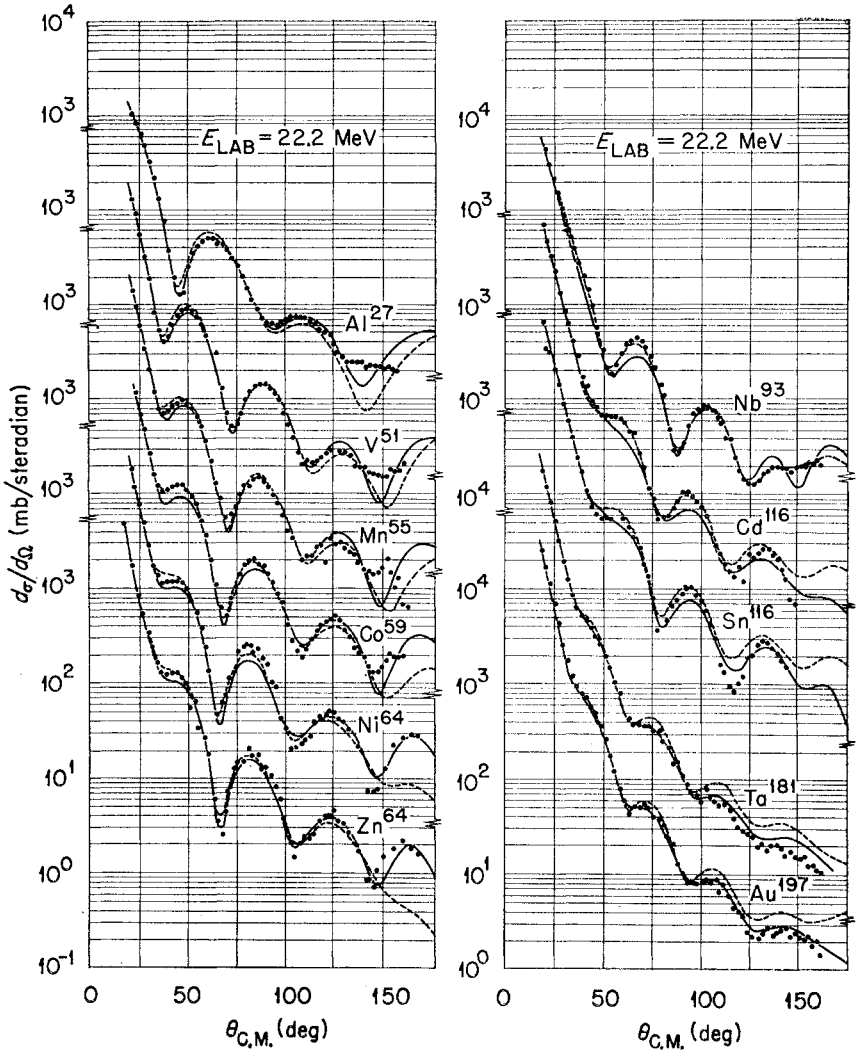

FIG. 18. Effect of volume imaginary potential on the fits to the 22.2-MeV data. The geometrical parameters are kept fixed to the values of Table V, the well depths V_S and W_D are adjusted for lowest χ^2 in each case. The dashed curves are for $W_S=0$ and the full curves are for $W_S=5$ MeV.

surface part of the imaginary potential continuously decreases as a function of energy but shows an increase with mass A. At 17 MeV and above, the analysis of the data becomes more sensitive to a volume absorption term, and there is, perhaps, some evidence that the volume part of the imaginary potential increases with energy. Analysis of data which cover a wide range of angles at higher energies would be valuable to settle this point. In Fig. 19 is given the shape of the imaginary potential for a light and heavy nucleus at both 17 and 22.2 MeV.

V. CONCLUSIONS

This analysis has shown that the optical model is able to fit the proton elastic-scattering differential cross sections to large scattering angles and still have a smooth dependence of its parameters as a function of mass number and energy. The dependence of the real well depth as a function of A seems to be reasonably well explained by a nuclear symmetry term in the potential and by the effect of the momentum dependence of the potential. The value of the coefficient of the nuclear symmetry term is not well determined but much evidence points to an average value of around 30 ± 10 MeV. The difference between the neutron and proton potential well depth can be accounted for by the nuclear symmetry term and the momentum dependence. Some fluctuations of the real potential well depth is seen to arise from the differences in core excitations in different nuclei. Those core excitations are also found to influence strongly the energy dependence of the well depth. The investigation of the effect of core excitations on the parameters of the optical model given in this paper was limited and more work remains to be done on this question. In view of the strong energy dependence of these effects, the formulas giving the real well depth is only expected to apply in the energy range studied, and should not be extrapolated to higher energy. How-

ever, below 20 MeV, it should be accurate enough to be useful in calculations using the distorted-wave Born approximation.

The polarization data are, in general, consistent with the analysis based on the elastic differential cross section alone. However, it would be interesting to have more data with both measurements taken on the same element, at the same energy, particularly in view of possible disagreement at large angles. For the reaction cross section, the same situation prevails, the data are in fair agreement with the calculations; however, in some cases the discrepancies may be significant, as for light nuclei at 10 MeV.

For the imaginary part of the potential, the situation is not as satisfactory as for the real part. It is possible to fit the data up to 17 MeV with only a surface imaginary potential; however, its depth increases as a function of A. There does not seem to be any indication of an increase in the surface imaginary potential as one goes to higher energy. If one allows both volume and surface imaginary potentials, then the fits are much improved at back angles for the 22-MeV data, but not appreciably changed at lower energies. The differences in core excitations in various nuclei give large fluctuations in the well depth. One may tentatively conclude that as the energy increases, the surface imaginary potential decreases and the volume imaginary potential increases being at most 3 MeV for 17-MeV protons and about 5 MeV for 22-MeV protons. It has not been possible to find out what is the optimum set of geometrical parameters to use in proton optical-model analysis but the set used for neutrons by Bjorklund and Fernbach was found satisfactory and convenient as it enables direct comparison of neutron and proton optical-model potentials.

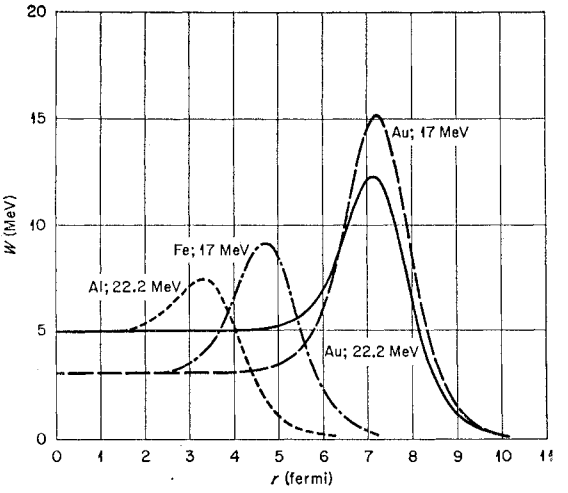

FIG. 19. Shapes of the imaginary potentials at 17 and 22 MeV for a light and heavy nucleus.

ACKNOWLEDGMENTS

It is a pleasure to thank Dr. G. R. Satchler and Dr. B. Buck for many discussions and comments on this work.